either K^+ and $(CH_3)_4N^+$ are both capable of binding to these macrocycles at very high cation concentrations or simply their presence leads to some unusual conformational effects. We conclude these NMR chemical shifts most likely arise from the very dramatic changes in ionic strength which occur in these solutions.

Acknowledgment. We thank the Meadows Foundation and the Robert A. Welch Foundation (Grant AT-584) for financial support.

Registry No. $H_4DOTEP{\cdot}2HCl$, 136705-17-4; H_4DOTEP, 136705-18-5; cyclen tetrahydrochloride, 10045-25-7.

Contribution from the Department of Chemistry and Molecular Structure Center, Indiana University, Bloomington, Indiana 47405

A Triangular Heterometallic Siloxide Containing Barium

Paul S. Coan, William E. Streib, and Kenneth G. Caulton*

Received April 5, 1991

Reaction of $KOSiPh_3$ with $Ba_3(OSiPh_3)_6(THF)$ in THF displaces barium from the triangular reagent to yield a colorless solid. Recrystallization in the presence of $MeOC_2H_4OMe$(DME) yields $KBa_2(OSiPh_3)_5(DME)_2$, characterized by ^1H and ^{29}Si NMR spectroscopy and X-ray diffraction. The molecule contains a triangular $KBa_2(\mu_3\text{-}OSiPh_3)_2(\mu_2\text{-}OSiPh_3)_3$ core with η^1- and η^2-DME ligation on each barium. The benzene-soluble molecule is fluxional in solution at both the $OSiPh_3$ and the DME groups. At −70 °C in CH_2Cl_2/C_6D_6, both η^1-DME/η^2-DME site exchange and intramolecular siloxide migration have been slowed, and the spectra are in agreement with retention of the solid-state structure in solution. Crystallographic data for $KBa_2(OSiPh_3)_5(DME)_2$ (−159 °C): $a = 15.474$ (3) Å, $b = 26.466$ (6) Å, $c = 23.783$ (5) Å, $\beta = 99.80$ (1)° with $Z = 4$ in space group $P2_1/n$.

Introduction

We have reported recently[1] that barium granules react with Ph_3SiOH in THF solvent only in the presence of NH_3 as a catalyst. After crystallization from toluene, the product has empirical formula $Ba(OSiPh_3)_2(THF)_{0.5}$. This molecule is actually a trimer which is noteworthy for having barium in coordination numbers 4 (once) and 5 (twice). The underlying feature it *shares* with many other trimetal species[2] is the $M_3(\mu_3\text{-}X)_2(\mu_2\text{-}X)_3$ core (A).

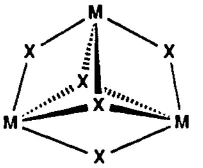

A

For the purposes of incorporating other metal ions (e.g. copper) into such a species, it would be useful to have an anionic barium siloxide (eq 1).[3] We therefore report here on our attempts to produce such an anionic barium synthon.

$$\mathrm{Ba}_n(\mathrm{OR})_m^- + \mathrm{CuCl}_2 \rightarrow \mathrm{ClCuBa}_n(\mathrm{OR})_m + \mathrm{Cl}^- \tag{1}$$

Experimental Section

Materials and Procedures. All manipulations were performed using standard Schlenk techniques either under an atmosphere of nitrogen or in a nitrogen-filled drybox. Toluene, pentane, hexanes, dimethoxyethane, and tetrahydrofuran were dried over potassium benzophenone ketyl, distilled under nitrogen, and subjected to freeze–pump–thaw cycles prior to use. The compound $Ba_3(OSiPh_3)_6(THF){\cdot}x THF$ was synthesized by a literature method.[1] $KOSiPh_3$ was synthesized[4] by addition of Ph_3SiOH to excess KH in toluene. The excess KH was filtered away and the solvent removed under vacuum to yield $KOSiPh_3$ as a colorless solid. Barium granules (Alfa) and triphenylsilanol (Aldrich) were used as received. Potassium hydride (Aldrich) was washed repeatedly with hexanes and dried under vacuum.

Table I. Crystallographic Data for $KBa_2(OSiPh_3)_5(DME)_2{\cdot}$hexane

chem formula	$C_{98}H_{95}Ba_2KO_9Si_5{\cdot}$solvent	fw	1871.03
a, Å	15.474 (3)	space group	$P2_1/n$
b, Å	26.466 (6)	T, °C	−159
c, Å	23.783 (5)	λ, Å	0.71069
β, deg	99.80 (1)	ρ_{calcd}, g cm^{-3}	1.295
V, Å^3	9597.97	μ(Mo K$_\alpha$), cm^{-1}	9.7
Z	4	R	0.0705
		R_w	0.0681

Physical Measurements. Hydrogen-1 NMR spectra were recorded on a Nicolet NT-360 spectrometer (360 MHz) and on a Bruker AM-500 spectrometer (500 MHz) and referenced to residual protons in the solvent. Silicon-29 NMR spectra were recorded on a Bruker AM-500 spectrometer (99.4 MHz) using an inverse-gated decoupling routine. Spectra were externally referenced to $SiMe_4$.

Synthesis of $KBa_2(OSiPh_3)_5(DME)_2$. $KOSiPh_3$ (0.315 g, 1.0 mmol) was combined with $Ba_3(OSiPh_3)_6(THF)$ (1.42 g, 0.667 mmol) in a Schlenk flask. THF (35 mL) was added to dissolve both solids, and the solution was stirred for 3 h at room temperature. The solution was concentrated under vacuum and layered with hexanes. Over the next several hours, colorless microcrystals formed. The solvent was removed via cannula. The microcrystals immediately lost solvent under vacuum and formed a white powder. Recrystallization from DME/hexanes gave colorless cubes. Yield: 0.990 g, 53%. ^1H NMR (C_6D_6 298 K): δ 7.68 (br, 30 H, ortho), 6.98 (m, 45 H, meta + para), 2.96 (s, DME), 2.79 (s, DME), 1.25 (m, hexanes), 1.18 (m, hexane), 0.88 (m, hexane). Note: The integrated intensity ratio of phenyl region to DME region varied from sample to sample. ^{29}Si NMR (C_6D_6, 298 K): δ −27.8 (br). Anal. Calcd for $C_{104}H_{109}Ba_2KO_9Si_5$: C, 63.82; H, 5.12. Found: C, 63.75; H, 5.59.

X-ray Structure Determination of $KBa_2(OSiPh_3)_5(DME)_2{\cdot}$hexane. A crystal of suitable size was mounted in a nitrogen atmosphere glovebag using silicone grease, and it was then transferred to a goniostat where it was cooled to −159 °C for characterization and data collection[5] (Table I). A search of a limited hemisphere of reciprocal space revealed intensities with Laue symmetry and systematic absences consistent with space group $P2_1/n$; this choice was later confirmed by the successful solution of the structure. Following complete data collection ($6° < 2\theta < 45°$), data processing gave a residual of 0.056 for the averaging of 1043 unique intensities which had been observed more than once. Four standards measured every 400 data showed no significant trends. No correction was made for absorption. The structure was solved using a combination of direct methods (MULTAN78) and Fourier techniques. The Ba positions were determined from an E map. The remaining non-hydrogen atoms were obtained from subsequent iterations of least-squares refinement and difference Fourier calculation. These included an elongated group of peaks assigned as a disordered molecule of hexane which

---

(1) Caulton, K. G.; Chisholm, M. H.; Drake, S. R.; Streib, W. E. *Angew. Chem., Int. Ed. Engl.* **1990**, *29*, 1483.

(2) For example: Evans, W. J.; Sollberger, M. S,; Hanusa, T. P. *J. Am. Chem. Soc.* **1988**, *110*, 1841.

(3) A copper/barium aggregate has been reported: Sauer, N. N.; Garcia, E.; Salazar, K. V.; Ryan, R. R.; Martin, J. A. *J. Am. Chem. Soc.* **1990**, *112*, 1524.

(4) McGeary, M. J.; Folting, K.; Streib, W. E.; Huffman, J. C.; Caulton, K. G. *Polyhedron*, in press.

(5) Huffman, J. C.; Lewis, L. N.; Caulton, K. G. *Inorg. Chem.* **1980**, *19*, 2755.

(6) McGeary, M. J.; Coan, P. S.; Folting, K.; Streib, W. E.; Caulton, K. G. *Inorg. Chem.* **1991**, *30*, 1723.

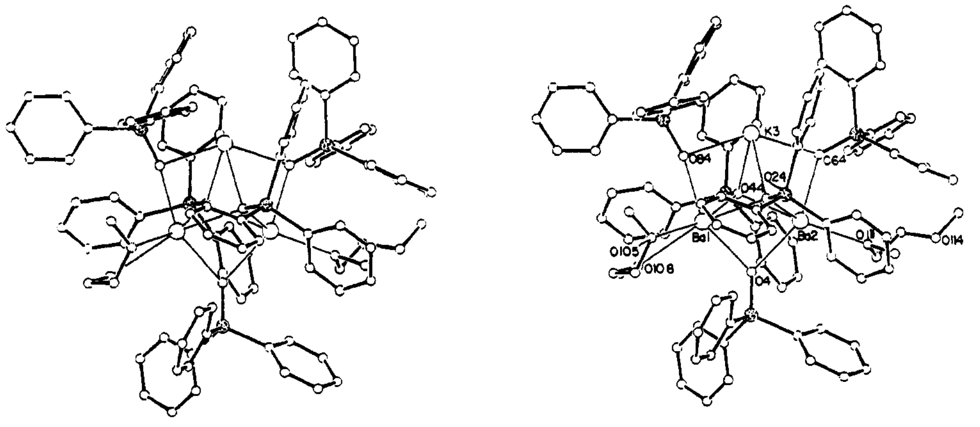

Figure 1. Stereo ORTEP drawing of the non-hydrogen atoms of $KBa_2(OSiPh_3)_5(DME)_2$ showing selected atom labeling. Silicons are stippled.

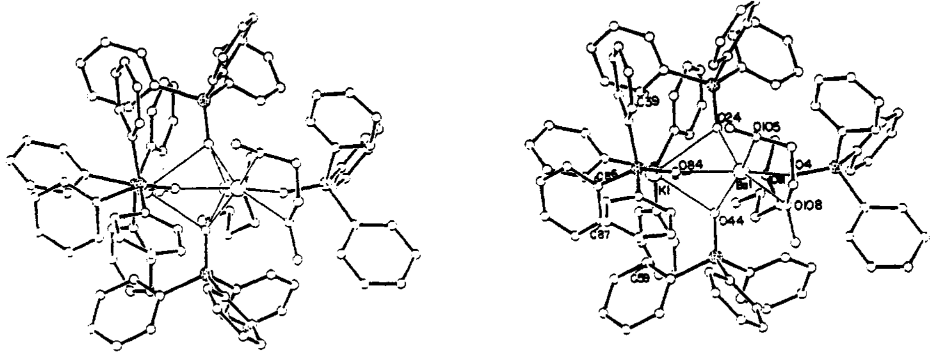

Figure 2. Stereo ORTEP drawing of the non-hydrogen atoms of $KBa_2(OSiPh_3)_5(DME)_2$, viewed along the edge of the KBa_2 plane. Ba(2) is eclipsed by Ba(1), and O(64) is eclipsed by O(84).

had been used as solvent. It was modeled as ten carbon atoms at half-occupancy. Hydrogens were included in fixed calculated positions on all carbons except in the disordered solvent. In the final cycles of least-squares refinement, the disordered solvent atoms were refined with isotropic thermal parameters and all other non-hydrogens were refined with anisotropic thermal parameters. The largest peak in the final difference map was a barium residual of 1.2 e/Å^3. The results of the structure determination are shown in Tables II and III and in Figure 1 and 2.

Results

(a) Synthesis of $KBa_2(OSiPh_3)_5(DME)_2$. The reaction of $KOSiPh_3$ with $Ba_3(OSiPh_3)_6(THF)$ (ratio 3:2) in THF yields colorless microcrystals. This material, probably a THF adduct, loses solvent immediately to generate a white powder. Recrystallization from DME/hexanes yields colorless cubes whose elemental analysis is consistent with the formula $KBa_2(OSiPh_3)_5(DME)_2$·hexane. When the reaction is carried out in a Ba:K ratio of 1:1, the major product is still the title compound. This material also loses solvent under vacuum (variable ^{1}H NMR integrations), but much more slowly than the proposed THF adduct. This is consistent with observations on a similar system.[6] $KBa_2(OSiPh_3)_5(DME)_2$ has some solubility in aromatic solvents but little in saturated hydrocarbons.

(b) Structure. The molecular structure (Figure 1 and 2) is based on the frequently encountered[2] triangular $M_3(\mu_2\text{-}OR)_3(\mu_3\text{-}OR)_2$ core. This is completed by *no* terminal ligands on K, a bidentate DME on a Ba(1), and a *monodentate* DME on Ba(2). The two barium metals thus have coordination numbers 6 (Ba(1)) and 5 (Ba(2)). Potassium has a low coordination number (4), and all of the donor atoms of these ligands occupy less than one hemisphere around the metal. Siloxide bonding is weaker to potassium than to barium, as judged by the fact that K–O distances (2.671 (7)–2.899 (7) Å) are *longer* than the corresponding distances to barium (2.523 (7)–2.681 (6) Å). The ionic radii of K^+ and Ba^{2+} are nearly identical. As a result of the disparity in crowding at four-coordinate potassium vs six-coordinate Ba(1), there is a significant bend about the (μ_2) O(84) (Figure 1) so as to move that $SiPh_3$ group toward K(3). Such bending is absent at O(64), between K(3) and the (five-coordinate) Ba(2). The μ_2-oxygens O(64) and O(84) are coplanar with their attached groups (angles sum to >358.3°), while there is some pyramidality (Figure 2) at O(4), between the two bariums (angles sum to 355.3°). All Si–O distances are identical to within 2σ.

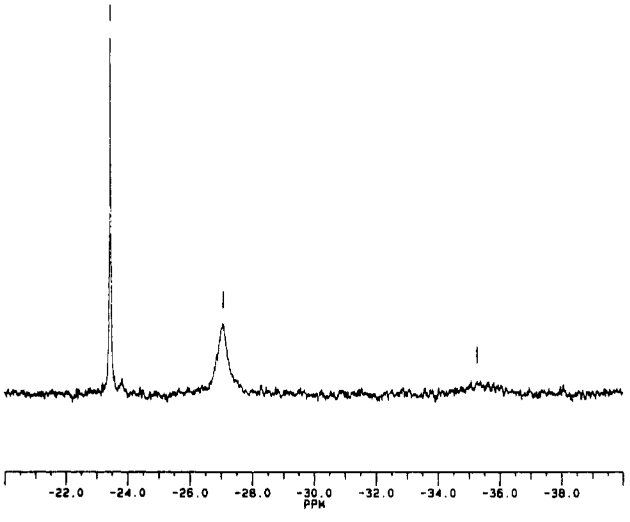

Figure 3. ^{29}Si NMR spectrum of $Ba_3(OSiPh_3)_6(THF)$.

Barium–O(siloxide) distances are not consistently longer to (six-coordinate) Ba(1) than to Ba(2), but the Ba–O(ether) distance to Ba(2) (2.826 (7) Å) is slightly shorter than that to Ba(1) (2.832 (7) and 2.919 (8) Å). The single ether oxygen on Ba(2) lies in the KBa_2 plane, while the two on Ba(1) lie out of this plane. It is of interest that the hexane molecule in the lattice does not lie near four-coordinate potassium, but instead is in the vicinity of the dangling tail of the η^1-DME ligand. The "open" hemisphere of potassium is generally shielded by phenyl rings from different siloxide groups. The shortest K/C distances (3.22 (1) and 3.25 (1) Å) are to the ipso (C(86) and ortho (C(87) carbons of the

Table II. Fractional Coordinates and Isotropic Thermal Parameters[a] for $KBa_2(OSiPh_3)_5(DME)_2$·hexane

	$10^4{}_y$	$10^4{}_y$	$10^4{}_z$	$10B_{iso}$
Ba(1)	6013.6 (4)	1075.7 (2)	7765.8 (2)	15
Ba(2)	7733.3 (4)	1093.3 (2)	6769.2 (2)	16
K(3)	8431 (1)	904 (1)	8335 (1)	19
O(4)	6014 (4)	1260 (2)	6651 (3)	16
Si(5)	5192 (2)	1235 (1)	6152 (1)	16
C(6)	4391 (6)	751 (4)	6325 (4)	15
C(7)	4670 (6)	333 (4)	6660 (4)	21
C(8)	4087 (7)	−19 (4)	6814 (5)	27
C(9)	3207 (7)	23 (4)	6615 (5)	32
C(10)	2904 (7)	423 (4)	6274 (5)	31
C(11)	3464 (7)	794 (4)	6133 (5)	25
C(12)	4576 (6)	1857 (4)	6034 (4)	21
C(13)	4654 (8)	2216 (4)	6454 (5)	30
C(14)	4166 (9)	2667 (5)	6363 (6)	46
C(15)	3603 (10)	2750 (6)	5871 (7)	54
C(16)	3500 (9)	2398 (6)	5445 (6)	54
C(17)	4009 (7)	1956 (4)	5531 (5)	31
C(18)	5508 (6)	1066 (4)	5442 (4)	17
C(19)	5049 (7)	723 (4)	5052 (4)	21
C(20)	5267 (7)	645 (4)	4518 (4)	26
C(21)	5945 (7)	907 (4)	4353 (4)	25
C(22)	6411 (7)	1249 (4)	4719 (5)	24
C(23)	6188 (6)	1332 (4)	5260 (4)	18
O(24)	7163 (4)	420 (2)	7463 (3)	19
Si(25)	7196 (2)	−178 (1)	7378 (1)	16
C(26)	6191 (6)	−535 (4)	7528 (4)	19
C(27)	5877 (7)	−460 (4)	8047 (5)	25
C(28)	5217 (7)	−759 (4)	8193 (5)	26
C(29)	4852 (7)	−1140 (4)	7828 (5)	30
C(30)	5142 (6)	−1225 (4)	7317 (5)	22
C(31)	5817 (7)	−934 (4)	7174 (5)	27
C(32)	7275 (6)	−338 (4)	6621 (4)	20
C(33)	6906 (6)	−26 (4)	6157 (4)	18
C(34)	6933 (7)	−146 (4)	5598 (4)	22
C(35)	7330 (8)	−587 (5)	5474 (4)	35
C(36)	7699 (9)	−910 (5)	5913 (5)	43
C(37)	7675 (7)	−783 (5)	6466 (5)	32
C(38)	8151 (7)	−492 (3)	7860 (4)	16
C(39)	8972 (7)	−249 (4)	7985 (4)	20
C(40)	9676 (6)	−475 (4)	8326 (5)	27
C(41)	9596 (6)	−954 (4)	8539 (5)	24
C(42)	8817 (7)	−1200 (4)	8411 (4)	22
C(43)	8104 (7)	−972 (4)	8085 (4)	24
O(44)	7476 (4)	1594 (2)	7684 (3)	20
Si(45)	7626 (2)	2191 (1)	7747 (1)	17
C(46)	6725 (6)	2520 (3)	8055 (4)	17
C(47)	6535 (7)	2363 (4)	8581 (4)	24
C(48)	5970 (7)	2640 (4)	8854 (5)	30
C(49)	5576 (7)	3066 (4)	8610 (5)	28
C(50)	5727 (6)	3224 (4)	8077 (5)	23
C(51)	6286 (7)	2953 (4)	7804 (5)	24
C(52)	7688 (6)	2477 (4)	7020 (4)	20
C(53)	7034 (6)	2360 (4)	6551 (4)	22
C(54)	7041 (7)	2559 (4)	6019 (5)	26
C(55)	7703 (8)	2887 (4)	5942 (4)	27
C(56)	8367 (7)	3011 (4)	6390 (5)	28
C(57)	8361 (7)	2805 (4)	6930 (4)	24
C(58)	8663 (6)	2376 (4)	8252 (4)	20
C(59)	9434 (7)	2107 (4)	8262 (5)	26
C(60)	10207 (6)	2252 (4)	8598 (5)	26
C(61)	10237 (8)	2673 (5)	8945 (5)	34
C(62)	9470 (8)	2946 (4)	8951 (5)	30
C(63)	8694 (6)	2799 (4)	8604 (5)	22
O(64)	9250 (4)	983 (2)	7380 (3)	19
Si(65)	10211 (2)	862 (1)	7251 (1)	17
C(66)	10219 (6)	378 (3)	6666 (4)	15
C(67)	9907 (9)	−101 (5)	6726 (5)	42
C(68)	9907 (10)	−463 (5)	6302 (6)	49
C(69)	10272 (8)	−372 (4)	5826 (4)	29
C(70)	10570 (7)	106 (5)	5749 (4)	27
C(71)	10546 (6)	477 (4)	6166 (4)	23
C(72)	10798 (7)	1447 (4)	7048 (4)	23
C(73)	11645 (7)	1426 (4)	6937 (5)	24
C(74)	12061 (7)	1850 (5)	6766 (5)	34
C(75)	11662 (8)	2314 (5)	6751 (5)	36
C(76)	10819 (8)	2350 (4)	6872 (5)	35
C(77)	10393 (7)	1920 (4)	7025 (4)	21
C(78)	10938 (6)	598 (4)	7907 (4)	19
C(79)	11530 (7)	207 (4)	7882 (5)	27
C(80)	12051 (7)	14 (5)	8370 (5)	33
C(81)	12011 (7)	234 (5)	8894 (6)	39
C(82)	11448 (9)	609 (5)	8936 (5)	40
C(83)	10918 (7)	806 (4)	8440 (5)	28
O(84)	6850 (4)	928 (2)	8759 (3)	20
Si(85)	7116 (2)	785 (1)	9414 (1)	17
C(86)	8316 (6)	936 (4)	9675 (4)	21
C(87)	8596 (7)	1433 (4)	9580 (4)	24
C(88)	9462 (7)	1574 (4)	9722 (5)	30
C(89)	10089 (7)	1231 (5)	9959 (5)	34
C(90)	9841 (7)	744 (5)	10057 (6)	39
C(91)	8950 (7)	594 (4)	9917 (5)	30
C(92)	6481 (6)	1161 (4)	9887 (4)	18
C(93)	6706 (7)	1157 (4)	10485 (5)	26
C(94)	6239 (8)	1424 (5)	10819 (5)	35
C(95)	5553 (8)	1716 (5)	10589 (6)	38
C(96)	5319 (7)	1748 (4)	10005 (6)	31
C(97)	5779 (7)	1461 (4)	9651 (4)	26
C(98)	6912 (6)	99 (4)	9555 (4)	20
C(99)	6222 (6)	−72 (4)	9818 (4)	20
C(100)	6041 (7)	−576 (4)	9868 (4)	24
C(101)	6574 (7)	−934 (4)	9687 (5)	25
C(102)	7270 (7)	−790 (4)	9433 (4)	28
C(103)	7446 (7)	−275 (4)	9360 (4)	23
C(104)	4564 (8)	431 (5)	8696 (5)	36
O(105)	4559 (5)	618 (3)	8142 (3)	32
C(106)	3750 (7)	839 (4)	7874 (5)	31
C(107)	3692 (7)	1362 (5)	8027 (6)	38
O(108)	4405 (5)	1631 (3)	7833 (4)	37
C(109)	4282 (9)	2162 (5)	7868 (6)	43
C(110)	8535 (7)	759 (4)	5445 (5)	29
O(111)	8518 (5)	1212 (3)	5788 (3)	30
C(112)	8699 (9)	1662 (5)	5500 (6)	39
C(113)	9667 (8)	1776 (5)	5524 (5)	36
O(114)	9994 (5)	1467 (3)	5128 (3)	33
C(115)	10915 (9)	1543 (6)	5176 (6)	52
C(116)	7851 (20)	2623 (11)	4222 (12)	44 (6)
C(117)	7949 (25)	2125 (16)	3889 (16)	65 (9)
C(118)	7442 (21)	2141 (12)	3506 (14)	53 (7)
C(119)	8106 (21)	1617 (12)	2762 (14)	54 (7)
C(120)	8306 (26)	1227 (15)	2321 (17)	75 (9)
C(121)	7954 (26)	1811 (17)	3598 (19)	77 (9)
C(122)	7784 (45)	2499 (27)	3972 (26)	132 (14)
C(123)	7437 (39)	1537 (27)	3040 (28)	119 (14)
C(124)	7864 (35)	1224 (22)	2553 (24)	113 (13)
C(125)	7758 (36)	1470 (25)	3217 (26)	104 (13)

[a] Isotropic values for those atoms refined anisotropically are calculated using the formula given by: Hamilton, W. C. *Acta Crystallogr.* **1959**, *12*, 609.

μ_2-$OSiPh_3$ group which bends away from the six-coordinate Ba(1), followed by 3.31 (1) (C (39) and 3.56 (1) Å (C(59)) distances to ortho carbons from the two different μ_3-$OSiPh_3$ groups. These are shown in Figure 2. Such distances are to be compared to the K/C distances in the graphite/potassium intercalate KC_8 (3.06 Å),[7] in (TMEDA)K(fluoreneide)[8] (3.04–3.68 Å), and in $KH_3Os(PMe_2Ph)_3$ (3.12–3.60 Å).[9] In $K_8(OSiPh_3)_8(DME)_3$, there is a K–C_{ipso} distance of 3.08 Å.[4]

(c) Spectra. The ^{29}Si NMR spectrum of $KBa_2(OSiPh_3)_5(DME)_2$ in C_6D_6 at 25 °C is a broad resonance (half-width ~1.5 ppm) at −27.8 ppm (compare the sharp singlet we have observed for $K_4(\mu_3$-$OSiPh_3)_4$ at −28.8 ppm). The ^1H NMR spectrum at

---

(7) Solin, S. A. *Adv. Chem. Phys.* **1982**, *49*, 455.

(8) Zerger, R.; Rhine, W.; Stucky, G. D. *J. Am. Chem. Soc.* **1974**, *96*, 5441.

(9) Huffman, J. C.; Green, M. A.; Kaiser, S. L.; Caulton, K. G. *J. Am. Chem. Soc.* **1985**, *107*, 5111.

Table III. Selected Bond Distances (Å) and Angles (deg) for $KBa_2(OSiPh_3)_5(DME)_2$

Ba(1)–K(3)	3.783 (2)	Ba(2)–O(24)	2.678 (6)
Ba(2)–K(3)	3.730 (2)	Ba(2)–O(44)	2.636 (6)
Ba(1)–O(4)	2.696 (6)	Ba(2)–O(64)	2.558 (6)
Ba(1)–O(24)	2.670 (6)	Ba(2)–O(111)	2.826 (7)
Ba(1)–O(44)	2.681 (6)	K(3)–O(24)	2.899 (7)
Ba(1)–O(84)	2.523 (7)	K(3)–O(44)	2.671 (7)
Ba(1)–O(105)	2.832 (7)	K(3)–O(64)	2.671 (7)
Ba(1)–O(108)	2.919 (8)	K(3)–O(64)	2.789 (7)
Ba(2)–O(4)	2.664 (6)	K(3)–O(84)	2.801 (6)
Ba(1)–K(3)–Ba(2)	61.71 (7)	O(64)–K(3)–O(84)	146.80 (20)
Ba(1)–Ba(2)–K(3)	58.82 (5)	Ba(1)–O(4)–Ba(2)	91.93 (19)
Ba(2)–Ba(1)–K(3)	58.47 (5)	Ba(1)–O(4)–Si(5)	126.4 (3)
O(4)–Ba(1)–O(24)	74.96 (19)	Ba(2)–O(4)–Si(5)	137.0 (4)
O(4)–Ba(1)–O(44)	72.23 (19)	Ba(1)–O(24)–Ba(2)	92.20 (20)
O(4)–Ba(1)–O(84)	149.61 (19)	Ba(1)–O(24)–K(3)	85.45 (18)
O(4)–Ba(1)–O(105)	121.42 (20)	Ba(1)–O(24)–Si(25)	135.6 (4)
O(4)–Ba(1)–O(108)	96.07 (21)	Ba(2)–O(24)–K(3)	83.85 (18)
O(24)–Ba(1)–O(44)	72.77 (20)	Ba(2)–O(24)–Si(25)	124.1 (3)
O(24)–Ba(1)–O(84)	83.83 (20)	K(3)–O(24)–Si(25)	119.7 (3)
O(24)–Ba(1)–O(105)	114.12 (21)	Ba(1)–O(44)–Ba(2)	92.90 (20)
O(24)–Ba(1)–O(108)	162.86 (22)	Ba(1)–O(44)–K(3)	89.95 (20)
O(44)–Ba(1)–O(84)	80.93 (20)	Ba(1)–O(44)–Si(45)	127.6 (4)
O(44)–Ba(1)–O(105)	165.40 (21)	Ba(2)–O(44)–K(3)	89.32 (21)
O(44)–Ba(1)–O(108)	118.97 (21)	Ba(2)–O(44)–Si(45)	122.2 (3)
O(84)–Ba(1)–O(105)	86.94 (21)	K(3)–O(44)–Si(45)	124.3 (3)
O(84)–Ba(1)–O(108)	109.48 (22)	Ba(2)–O(64)–K(3)	88.35 (19)
O(105)–Ba(1)–O(108)	57.83 (22)	Ba(2)–O(64)–Si(65)	134.9 (4)
O(4)–Ba(2)–O(24)	75.37 (19)	K(3)–O(64)–Si(65)	135.0 (4)
O(4)–Ba(2)–O(44)	73.45 (19)	Ba(1)–O(84)–K(3)	90.40 (21)
O(4)–Ba(2)–O(64)	151.88 (20)	Ba(1)–O(84)–Si(85)	164.0 (4)
O(4)–Ba(2)–O(111)	117.16 (20)	K(3)–O(84)–Si(85)	104.6 (3)
O(24)–Ba(2)–O(44)	73.37 (20)	Ba(1)–O(105)–C(104)	124.6 (6)
O(24)–Ba(2)–O(64)	86.58 (20)	Ba(1)–O(105)–C(106)	111.5 (6)
O(24)–Ba(2)–O(111)	144.65 (20)	C(104)–O(105)–C(106)	115.2 (9)
O(44)–Ba(2)–O(64)	80.88 (20)	Ba(1)–O(108)–C(107)	118.1 (6)
O(44)–Ba(2)–O(111)	140.61 (21)	Ba(1)–O(108)–C(109)	128.6 (7)
O(64)–Ba(2)–O(111)	90.01 (21)	C(107)–O(108)–C(109)	110.5 (9)
O(24)–K(3)–O(44)	69.34 (19)	Ba(2)–O(111)–C(110)	115.1 (6)
O(24)–K(3)–O(64)	78.27 (19)	Ba(2)–O(111)–C(112)	129.6 (6)
O(24)–K(3)–O(84)	74.99 (19)	C(110)–O(111)–C(112)	113.3 (8)
O(44)–K(3)–O(64)	76.17 (20)	C(113)–O(114)–C(115)	109.5 (10)
O(44)–K(3)–O(84)	76.22 (20)		

25 °C in C_6D_6 shows only one type of phenyl ring and one singlet each for the CH_2 and CH_3 protons of DME. A rapid $\eta^1 \rightleftarrows \eta^2$ exchange of DME ligands and a *global* exchange among the $OSiPh_3$ groups are indicated by these ^1H NMR data.

For comparison, the ^{29}Si NMR spectrum (25 °C) of $Ba_3(OSiPh_3)_6(THF)\cdot x THF$ (I) in CH_2Cl_2/C_6D_6 (80:20) is shown in figure 3. These resonances integrate 2:3:1.[10] We have evidence[11] that the ^{29}Si chemical shift moves downfield as the siloxide goes from terminal to μ_2 to μ_3 sites. Thus, we assign the sharp singlet in Figure 3 to the two nonfluxional μ_3-$OSiPh_3$ groups, the *broad* intensity 3 resonance to the coalescing inequivalent μ_2-$OSiPh_3$ groups, and the extremely broad, intensity 1 resonance to the terminal siloxide as it begins to exchange with the μ_2 groups. The more facile site exchange between the terminal and double bridging groups is consistent with trends seen in metal carbonyl cluster chemistry and also with the availability of an open terminal site at Ba* in the ground-state structure. Certain of our ^{29}Si NMR spectra of this molecule also show variations in the line width of the upfield resonance which correlate with the amount (*x* above) of excess (i.e., lattice) THF. This is consistent with the fact that THF must ultimately migrate to give global siloxide site exchange.

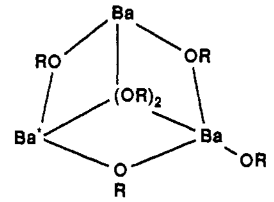

I

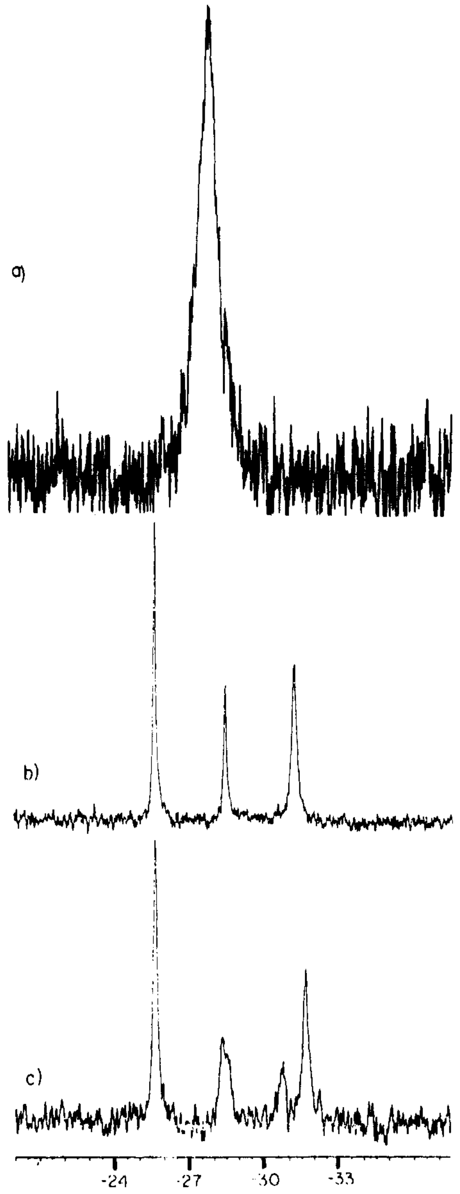

Figure 4. Variable-temperature ^{29}Si NMR spectra of $KBa_2(OSiPh_3)_5(DME)_2$ in 4:1 CH_2Cl_2/C_6D_6: (a) 25 °C; (b) -50 °C; (c) -70 °C.

The 99.4-MHz ^{29}Si NMR spectrum of $KBa_2(OSiPh_3)_5(DME)_2$ shows only a single broad line at 25 °C in toluene (Figure 4). The half-width is 1 ppm. At -50 °C in 4:1 CH_2Cl_2/C_6D_6, the ^{29}Si NMR spectrum has resolved into three lines, of intensity 2:1:2, assigned to the μ_3-OR, Ba–(μ_2-OR)–Ba, and K–(μ_2-OR)–Ba sites under the condition of rapid interchange of the η^2- and η^1-DME binding modes (eq 2). At -70 °C (Figure 4), the spectrum resolves into four lines, of intensity 2:1:1:1, consistent with either structure in eq 2 and near cessation (on the NMR time scale) of the η^2-DME/η^1-DME exchange process. An effective mirror plane still exists, however, to make the two μ_3-$OSiPh_3$ groups

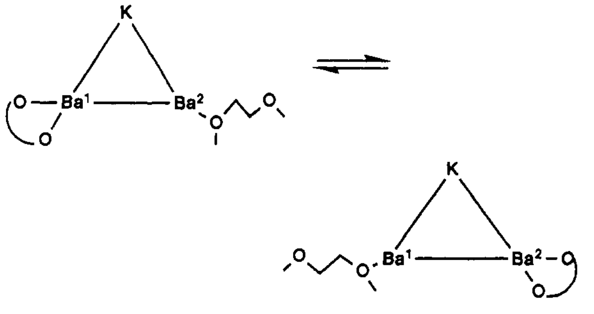

(2)

---

[10] In ref 1, we failed to detect the very broad resonance at -35.5 ppm.

[11] Coan, P. S.; McGeary, M. J.; Lobkovsky, E.; Caulton, K. G. *Inorg. Chem.* **1991**, *30*, 3570. Apblett, A. W.; Cheatham, L. K.; Barron, A. R. *J. Mater. Sci.* **1991**, *1*, 143.

equivalent.[12] Since all of these dynamic processes occur in hydrocarbon solvent, we prefer an intramolecular $OSiPh_3$ migration mechanism to any dissociation of Ph_3SiO^-. These spectra also establish that the solid-state structure is maintained in benzene or CH_2Cl_2 solution.

Discussion

The structure reported here for $KBa_2(OSiPh_3)_5(DME)_2$ shares some features with that of $Ba_3(OSiPh_3)_6(THF)$ (see B and C).

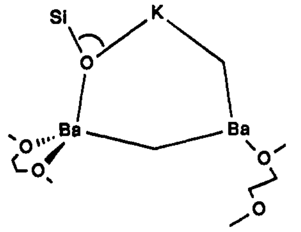

B

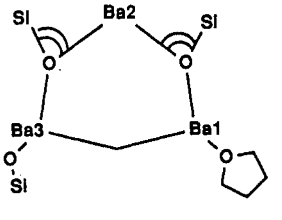

C

Both have the $M_3(\mu_3\text{-}X)_2(\mu_2\text{-}X)_3$ core. Ba(2) in C plays the role of K in B in being only four-coordinate. Since C contains one more $OSiPh_3$ ligand than does B, this ligand occupies one terminal position (at Ba(3)). The corresponding metal in B is coordinated by η^2-DME. The remaining barium in each molecule coordinates only one ether oxygen. The only difference between B and C is that two μ_2-$OSiPh_3$ groups bend toward the four-coordinate metal in C, while only one of them does in B.

The observed reaction of $KOSiPh_3$ with $Ba_3(OSiPh_3)_6(THF)$ is surprising (or at least unpredictable), since it would seem destined to *add* the siloxide nucleophile to the intact Ba_3 triangle. Products such as the potassium salt of $Ba_3(OSiPh_3)_7(THF)_n^-$ might have been anticipated. Instead, there is a major reorganization of the Ba_3 triangle, one barium and two siloxides are lost, and the resulting siloxide-rich $Ba_2(OSiPh_3)_5^-$ species sequesters K^+. The apparent guiding theme is that the chemistry is dominated by the formation of (uncharged) *molecular* species, to the exclusion of (charge-separated) salts.

Acknowledgment. This work was supported by the Department of Energy. We thank Scott Horn for skilled technical assistance.

Registry No. $KBa_2(OSiPh_3)_3(DME)_2$·hexane (coordination compound entry), 137540-23-9; $KOSiPh_3$, 25221-22-1; Ph_3SiOH, 791-31-1; $KBa_2(OSiPh_3)_5(DME)_2$·hexane (salt entry), 137540-25-1.

Supplementary Material Available: Tables giving full crystallographic details and anisotropic thermal parameters (4 pages); a listing of calculated and observed structure factors (25 pages). Ordering information is given on any current masthead page.

---

(12) At −80 °C, the ^{29}Si NMR spectrum further resolves into a total of seven lines. This we assign to freezing out of two conformers, as a result of the crowded nature of the molecule.

Contribution from the Department of Chemistry, University of New Hampshire, Durham, New Hampshire 03824-3598, and Institute for Inorganic Chemistry, University of Witten/Herdecke, Stockumer Strasse 10, 5810 Witten, Germany

Oxidation of Dihydroxy Aromatic Substrates by Hexachloroiridate(IV). Mechanistic Information from Volumes of Activation

C. D. Hubbard,*,[1a] A. Gerhard,[1b] and R. van Eldik*,[1b]

Received June 16, 1991

The reaction between the hexachloroiridate(IV) ion and several benzenediols has been studied kinetically in aqueous perchloric acid solution at pressures up to 100 MPa. The volumes of activation are almost independent of the aromatic substituent at a given temperature and acidity and are all within the range −20 to −30 $cm^3\ mol^{-1}$. Encounter complex (ion–molecule) formation is followed by rate-determining electron transfer according to an outer-sphere electron-transfer mechanism. The latter step involves significant charge creation with consequent increasing solvent electrostriction and accounts principally for the significantly negative ΔV^* data. The results are compared with those for related systems recently reported in the literature.

Introduction

The subject of oxidation of dihydroxy aromatic compounds by metal complexes during which a quinone is produced has received considerable attention in recent years.[2-5] The redox chemistry of diol–quinone systems has its own intrinsic interest, but the identification of ubiquinone (a 1,4-quinone with a lengthy hydrocarbon chain in the 3-position), in conjunction with a metal center, as an electron acceptor in photosynthetic bacterial action has led to widespread additional interest[6] in these types of reactions. We are generally interested in the detailed redox mechanism for the oxidation of a benzenediol to a quinone by simple metal ions or complexes as oxidants. We have recently studied the oxidation of catechol, the 4-*tert*-butyl derivative of catechol, and methyl-1,4-hydroquinone by $Fe(CN)_4(bpy)^-$ in more detail.[7] The reactions were all characterized by strongly negative volumes of activation, a finding which was ascribed to the dominance of electrostriction of the solvent due to increasing charge development in forming the transition state for the overall redox reaction in (I). Another interesting aspect of these systems is the fact that

$$2Fe(CN)_4(bpy)^- + QH_2 \rightarrow 2Fe(CN)_4(bpy)^{2-} + 2H^+ + Q \quad (I)$$

the rate-determining electron-transfer step is a nonsymmetrical outer-sphere reaction in which one of the reaction partners is a neutral species. The pressure dependence of the kinetics of several other comparable redox reactions has been studied in detail recently.[8-12] We have therefore extended our earlier work[7] to a series of dihydroxy aromatic substrates and investigated the pressure dependence of their oxidation by hexachloroiridate(IV), $IrCl_6^{2-}$. The ambient-pressure kinetics of the oxidation of benzenediols and other substrates by the $IrCl_6^{2-}$ ion have been investigated in some detail both in water[4] and in mixed aqueous solvents.[12] By application of Marcus' theory the kinetics in aqueous

---

(1) (a) University of New Hampshire. (b) University of Witten/Herdecke.
(2) Pelizzetti, E.; Mentasti, E.; Pramauro, E. *J. Chem. Soc., Dalton Trans.* **1976**, 23.
(3) Pelizzetti, E.; Mentasti, E. *J. Chem. Soc., Dalton Trans.* **1976**, 2222.
(4) Mentasti, E.; Pelizzetti, E.; Baiocchi, C. *J. Chem. Soc., Dalton Trans.* **1977**, 132.
(5) Pelizzetti, E.; Mentasti, E.; Baiocchi, C. *J. Phys. Chem.* **1976**, *80*, 2979.
(6) Norris, J. R.; Schiffer, M. *Chem. Eng. News* **1990**, *68* (July 30), 22; **1990**, *68* (Oct 8), 27. McAuley, A.; Whitcombe, T. W. In *Mechanisms of Inorganic and Organometallic Reactions*; Twigg, M. V., Ed.; Plenum: New York, 1989; Vol. 6, Chapter 3.
(7) Hubbard, C. D.; Bajaj, H. C.; van Eldik, R.; Burgess, J.; Blundell, N. J. *Inorg. Chim. Acta* **1991**, *183*, 1.
(8) Murguia, M. A.; Wherland, S. *Inorg. Chem.* **1991**, *30*, 139.
(9) Anderson, K. A.; Wherland, S. *Inorg. Chem.* **1991**, *30*, 624.
(10) Bänsch, B.; Martinez, P.; Uribe, D.; Zuluaga, J.; van Eldik, R. *Inorg. Chem.*, in press.
(11) Bänsch, B.; Martinez, P.; van Eldik, R. *J. Phys. Chem.*, in press.
(12) Minero, C.; Pramauro, E.; Pelizzetti, E.; Blundell, N. J.; Burgess, J.; Radulovic, S. *Inorg. Chim. Acta* **1990**, *173*, 43.